UC Davis
UC Davis Previously Published Works

Title

Interlayer antisynchronization in degree-biased duplex networks.

Permalink

https://escholarship.org/uc/item/91q6r1zb

Journal

Physical review. E, 107(3-1)

ISSN

2470-0045

Authors

Nag Chowdhury, Sayantan
Rakshit, Sarbendu
Hens, Chittaranjan
et al.

Publication Date

2023-03-01

DOI

10.1103/physreve.107.034313

Peer reviewed

Interlayer antisynchronization in degree-biased duplex networks

Sayantan Nag Chowdhury [1,2,*] Sarbendu Rakshit [3,†] Chittaranjan Hens [4,‡] and Dibakar Ghosh [5,§]

[1]*Department of Environmental Science and Policy, University of California, Davis, California 95616, USA*
[2]*Technology Innovation Hub (TIH), IDEAS (Institute of Data Engineering Analytics and Science Foundation),*
Indian Statistical Institute, 203 B. T. Road, Kolkata 700108, India
[3]*Department of Mechanical Engineering, University of California, Riverside, California 92521, USA*
[4]*Center for Computational Natural Sciences and Bioinformatics, International Institute of Information Technology,*
Gachibowli, Hyderabad 500032, India
[5]*Physics and Applied Mathematics Unit, Indian Statistical Institute, 203 B. T. Road, Kolkata 700108, India*

With synchronization being one of nature's most ubiquitous collective behaviors, the field of network synchronization has experienced tremendous growth, leading to significant theoretical developments. However, most previous studies consider uniform connection weights and undirected networks with positive coupling. In the present article, we incorporate the asymmetry in a two-layer multiplex network by assigning the ratio of the adjacent nodes' degrees as the weights to the intralayer edges. Despite the presence of degree-biased weighting mechanism and attractive-repulsive coupling strengths, we are able to find the necessary conditions for intralayer synchronization and interlayer antisynchronization and test whether these two macroscopic states can withstand demultiplexing in a network. During the occurrence of these two states, we analytically calculate the oscillator's amplitude. In addition to deriving the local stability conditions for interlayer antisynchronization via the master stability function approach, we also construct a suitable Lyapunov function to determine a sufficient condition for global stability. We provide numerical evidence to show the necessity of negative interlayer coupling strength for the occurrence of antisynchronization, and such repulsive interlayer coupling coefficients cannot destroy intralayer synchronization.

I. INTRODUCTION

Multilayer networks [1–3] of coupled oscillators provide a fascinating platform to study the collective asymptotic behavior of dynamical systems evolving on top of it. Several layers of such a network prove to be a fertile playground to reveal the interplay between the network structure and the unfolding of collective phenomena of various dynamical processes. The hallmark property of a realistic system is the complex connectivity patterns of its components, and it may often give rise to complex dynamics. An isolated network can seldom describe such collective dynamics of interconnected systems. Thus, researchers often resort to multilayer networks anticipating some new fresh insights into complex systems. In past years, numerous studies have unfolded several emergent collective phenomena, such as extreme events [4,5], percolation [6,7], congestion of traffic [8,9], epidemics spreading [10,11], controllability [12], evolutionary game dynamics [13,14], and diffusion [15], to name a few. The results presented in these studies demonstrate a very different phenomenology from the one found in monolayer networks. Various complex forms of synchronized dynamics of multilayer networks of the coupled oscillator, such as interlayer synchronization [16,17], relay

synchronization [18], antiphase synchronization [19], relay interlayer synchronization [20], intralayer synchronization [21–23], cluster synchronization [24,25], explosive synchronization [26–28], breathing synchronization [29], solitary states [30], and complete synchronization [31], have been brought to the limelight by investigating the role that network structure plays in the onset and stability of such coherent states. Nevertheless, the study of interlayer antisynchronization on multilayer structures remains relatively unexplored to the best of our knowledge under different contexts.

Interlayer antisynchronization in a multiplex network refers to the dynamical process where two identical oscillators directly connected through the interlayer link settle down to an equal amplitude with a constant phase difference of π. Inspired by antiphase patterns in two-module neuronal networks [32], we are interested in deriving the criteria for the existence and stability of interlayer antisynchronization state in a duplex (multiplex with two layers). Apart from performing local stability analysis of this state of the interacting systems with the help of the master stability function (MSF) approach [33,34], we are equally interested in deriving the sufficient condition for global stability of the interlayer antisynchronization state. To do this, we construct a suitable Lyapunov function for deriving the global stability of this state. The term "global stability" here reflects that the system will evolve into the interlayer antisynchronization state irrespective of the chosen initial conditions except for a set of measure zero [35].

Most of the previous investigations on the synchronization [36–41] of complex networks of coupled dynamical systems

*jcjeetchowdhury1@gmail.com
†sarbendu.math@gmail.com
‡chittaranjanhens@gmail.com
§dibakar@isical.ac.in

are performed by assuming (i) unweighted and undirected networks and (ii) attractive (positive) coupling strengths only. However, realistic systems are far more complicated, and there are ample real-life examples where heterogeneous connectivity weights [42] and the simultaneous presence of attractive-repulsive interactions [43–47] are beneficial in portraying real-world scenarios. For instance, the number of emails exchanged between two colleagues in an organization, and the number of scientific collaborations between two scientists depend on different contexts. It is best to assign a weight to each edge of the network to derive relationships between such interacting individuals. Instead of using the random weighted directed network, we consider the influence of a node's degree on its neighbors and construct a degree-biased network to study the interlayer antisynchronization and intralayer synchronization in the multiplex. Synchronization on weighted networks have been studied extensively in the literature, as indicated in Refs. [48–52]. Nevertheless, to our knowledge, the emergence and (local and global) stability of interlayer antisynchronization on multiplex networks with weighted intralayer connections have never been investigated. Furthermore, we introduce the negative interlayer coupling strength, which is found to be essential for the onset of the interlayer antisynchronization as per our numerical simulations. The positive intralayer coupling strengths allow the system to settle into the intralayer synchronization, despite the presence of negative interlayer coupling strength. Numerous real-life scenarios are highlighted in the review [53] to emphasize the importance of attractive-repulsive interaction. As per Ref. [54], all the pairs of interacting subunits of a system can not minimize their energy due to opposing coupling strengths. When network connections change over time, such temporal networks with positive-negative coupling may produce several peculiar states like static π state [55], extreme events [56,57], inhomogeneous small oscillation [58], and many more. Ecologists and data analysts also unveil the tug of war between positive and negative interactions for extracting useful information about ecosystems' diversity in species [59,60].

Following the seminal works by Estrada and his collaborators [61,62], we consider three distinct types of intralayer networks: hub-attracting, hub-repelling, and unweighted network. We furnish analytical insights about the conditions for the emergence of intralayer synchronization and interlayer antisynchronization. We analytically derive the necessary conditions for all the identical oscillators to evolve in unison within the layers. All these analytical results help to design a duplex with suitable oscillators and couplings that allows the system to achieve such coherent states. Our numerical simulations also support that our analytical findings (existence and stability criteria) effectively help to achieve intralayer synchronization and interlayer antisynchronization when appropriate conditions are met.

II. MATHEMATICAL MODEL

To illustrate our findings, we consider a multiplex network with two layers. On top of the vertices of each layer consisting of N nodes, we place an m-dimensional identical dynamical system with state vectors $\mathbf{x}_{\alpha,i} \in \mathbb{R}^m$, $\alpha = 1, 2$ and $i = 1, 2, 3, \ldots, N$. Here the first component (α) of the suffices

of $\mathbf{x}_{\alpha,i}$ represents the number of the layer, and the second component (i) depicts the number of the node of the αth layer. Each of these isolated oscillators maintains the dynamical equations in the absence of intralayer and interlayer couplings as follows:

$$\dot{\mathbf{x}}_{\alpha,i} = f(\mathbf{x}_{\alpha,i}), \quad (1)$$

where $f:\mathbb{R}^m \to \mathbb{R}^m$ is the autonomous nonlinear evolution function. We assume this f is continuously differentiable with respect to its argument. We need to consider this assumption, which we need later for performing the stability analysis. Let $\mathscr{A}_{ij}^{[\alpha]}$, $\alpha = 1, 2$ be the elements of the adjacency matrix encoding the intralayer topology of the αth layer. Precisely, for $\alpha = 1, 2$,

$$\mathscr{A}_{ij}^{[\alpha]} = \begin{cases} 1, & \text{if } i\text{th and } j\text{th nodes are connected in the } \alpha\text{th layer} \\ 0, & \text{otherwise} \end{cases}. \quad (2)$$

Since we are also interested in inspecting intralayer synchronization, we only consider connected intralayer networks. When both the layers are coupled, then we can describe the dynamical evolution of the ith node of the αth layer as follows:

$$\dot{\mathbf{x}}_{1,i} = f(\mathbf{x}_{1,i}) + k_A \sum_{j=1}^{N} \tilde{\mathscr{A}}_{ij}^{[1]} G[\mathbf{x}_{1,j}, \mathbf{x}_{1,i}] + k_R H[\mathbf{x}_{2,i}, \mathbf{x}_{1,i}],$$

$$\dot{\mathbf{x}}_{2,i} = f(\mathbf{x}_{2,i}) + k_A \sum_{j=1}^{N} \tilde{\mathscr{A}}_{ij}^{[2]} G[\mathbf{x}_{2,j}, \mathbf{x}_{2,i}] + k_R H[\mathbf{x}_{1,i}, \mathbf{x}_{2,i}]. \quad (3)$$

Here $\tilde{\mathscr{A}}_{ij}^{[\alpha]}$ is generated by assigning a weight to each element $\mathscr{A}_{ij}^{[\alpha]}$ as

$$\tilde{\mathscr{A}}_{ij}^{[\alpha]} = \left(\frac{d_j}{d_i}\right)^{\beta} \mathscr{A}_{ij}^{[\alpha]}, \quad (4)$$

where $\beta \in \{0, 1, -1\}$ and d_i denotes the degree of the ith node in the whole multiplex network whose adjacency matrix is given by

$$\mathscr{A} = \begin{pmatrix} \mathscr{A}^{[1]} & I \\ I & \mathscr{A}^{[2]} \end{pmatrix}. \quad (5)$$

Here I is the identity matrix of order N. When $\beta = +1$, we have a hub-attracting intralayer adjacency matrix by adopting the terminology from Ref. [62]. This rescaled unsymmetric hub-attracting matrix reflects the tendency to produce a strong influence on the low-degree neighbors by the high-degree nodes [63]. We can inspect the reverse scenario of biased domination from low to high-degree nodes with the hub-repelling matrix by considering $\beta = -1$ [61,63]. However, the matrix remains unaltered for $\beta = 0$, i.e., we have $\tilde{\mathscr{A}}_{ij}^{[\alpha]} = \mathscr{A}_{ij}^{[\alpha]}$ for $\beta = 0$. Thus, Eq. (3) reduces to

$$\dot{\mathbf{x}}_{1,i} = f(\mathbf{x}_{1,i}) + k_A \sum_{j=1}^{N} \left(\frac{d_j}{d_i}\right)^{\beta} \mathscr{A}_{ij}^{[1]} G[\mathbf{x}_{1,j}, \mathbf{x}_{1,i}]$$
$$+ k_R H[\mathbf{x}_{2,i}, \mathbf{x}_{1,i}],$$

$$\dot{\mathbf{x}}_{2,i} = f(\mathbf{x}_{2,i}) + k_A \sum_{j=1}^{N} \left(\frac{d_j}{d_i}\right)^{\beta} \mathscr{A}_{ij}^{[2]} G[\mathbf{x}_{2,j}, \mathbf{x}_{2,i}]$$

$$+ k_R H[\mathbf{x}_{1,i}, \mathbf{x}_{2,i}]. \tag{6}$$

Here k_A is the intralayer coupling strength, and $G : \mathbb{R}^m \times \mathbb{R}^m \to \mathbb{R}^m$ is the output vectorial function within the layers. On the other hand, k_R is the interlayer coupling strength, and $H:\mathbb{R}^m \times \mathbb{R}^m \to \mathbb{R}^m$ is the interlayer coupling vectorial function. In the next section, we rigorously investigate the necessary criteria for the existence of interlayer antisynchronization state and intralayer synchronization.

III. ANALYTICAL FINDINGS

Before representing our key analytical findings, first, we briefly define two synchronized states: (i) interlayer antisynchronization and (ii) intralayer synchronization states.

The interlayer antisynchronization depicts the synchronous time evolution of the oscillators situated on top of the replica nodes with a constant phase difference of π, i.e., the sum $[\mathbf{x}_{1,i}(t) + \mathbf{x}_{2,i}(t)]$ of the dynamics of the state variables of the ith oscillators of both layers vanishes after the transient. Mathematically, when the system evolves in the interlayer antisynchronization state, we have

$$\mathbf{x}_{1,i}(t) + \mathbf{x}_{2,i}(t) = \mathbf{0}, \quad \forall \quad i = 1, 2, \ldots, N. \tag{7}$$

We define the interlayer antisynchronization error as

$$E = \lim_{t \to \infty} \frac{1}{T} \int_{t}^{t+T} \sum_{i=1}^{N} \frac{\|\mathbf{x}_{1,i}(t) + \mathbf{x}_{2,i}(t)\|}{N} \, d\tau. \tag{8}$$

Clearly, E necessarily becomes zero in the state of interlayer antisynchronization and remains nonzero otherwise.

On the other hand, intralayer synchronization remains completely independent of the interlayer antisynchronization. A system may evolve in the interlayer antisynchronization state; however, it may not maintain the intralayer synchronization and vice versa. Intralayer synchronization refers to the synchronous evolution of all dynamical units within each layer. In other words, proceeding to the limit as $t \to \infty$ for all $i = 1, 2, \ldots, N$ and $\alpha = 1, 2$, there definitely exists intralayer synchronization solution $\mathbf{x}_\alpha(t) \in \mathbb{R}^m$ such that

$$\mathbf{x}_{\alpha,i}(t) \to \mathbf{x}_\alpha(t). \tag{9}$$

Now we move on to prove the necessary conditions on the individual node dynamics f, the network topology $\mathscr{A}_{ij}^{[\alpha]}$, the coupling functions G and H for the emergence of interlayer antisynchronization and intralayer synchronization states.

A. Necessary condition for interlayer anti synchronization state

When the system evolves in the interlayer antisynchronization state, all the vertices of one layer maintain the same amplitude with its replica nodes of the different layers. Still their phase difference will be π. Thus, using Eq. (7), we obtain

the following set of equations from Eq. (3) as follows:

$$\dot{\mathbf{x}}_{1,i} = f(\mathbf{x}_{1,i}) + k_A \sum_{j=1}^{N} \tilde{\mathscr{A}}_{ij}^{[1]} G[\mathbf{x}_{1,j}, \mathbf{x}_{1,i}]$$

$$+ k_R H[-\mathbf{x}_{1,i}, \mathbf{x}_{1,i}],$$

$$\dot{\mathbf{x}}_{1,i} = -f(-\mathbf{x}_{1,i}) - k_A \sum_{j=1}^{N} \tilde{\mathscr{A}}_{ij}^{[2]} G[-\mathbf{x}_{1,j}, -\mathbf{x}_{1,i}]$$

$$- k_R H[\mathbf{x}_{1,i}, -\mathbf{x}_{1,i}]. \tag{10}$$

These equations remain consistent if
(1) $f(\mathbf{x}) = -f(-\mathbf{x})$, i.e., f is an odd function
(2) $\sum_{j=1}^{N} \tilde{\mathscr{A}}_{ij}^{[1]} G[\mathbf{x}_{1,j}, \mathbf{x}_{1,i}] = -\sum_{j=1}^{N} \tilde{\mathscr{A}}_{ij}^{[2]} G[-\mathbf{x}_{1,j}, -\mathbf{x}_{1,i}]$
and

(3) $H(-\mathbf{x}, \mathbf{x}) = -H(\mathbf{x}, -\mathbf{x})$, i.e., H is an odd function.

These three conditions are necessary for obtaining interlayer antisynchronization and, by no means, sufficient ones. Mere fulfilling these three conditions, one can not anticipate interlayer antisynchronization.

B. Necessary condition for intralayer synchronization

Let all the trajectories of the first layer maintain a coherent rhythm, i.e., $\mathbf{x}_{1,i}(t)$ converges to $\mathbf{x}_1(t)$ at some time, say, $t = t_1$. Similarly, $\mathbf{x}_{2,i}(t)$ of the second layer converges to $\mathbf{x}_2(t)$ at some time $t = t_2$. Let t_0 be the maximum of $\{t_1, t_2\}$. Thus, for any time $t \geqslant t_0$, the rate of changes of all the state variables in all respective layers should be identical. The system converges into the intralayer synchronization manifold $(\mathbf{x}_1(t), \mathbf{x}_2(t))$ for $t \geqslant t_0$.

Without loss of any generality, we choose two arbitrary nodes i and l (say) from both the layers. Therefore, we have $\mathbf{x}_{1,i}(t) = \mathbf{x}_{1,l}(t) = \mathbf{x}_1(t)$ and $\mathbf{x}_{2,i}(t) = \mathbf{x}_{2,l}(t) = \mathbf{x}_2(t)$, once the system (3) settles into the intralayer synchronization manifold. Then the corresponding dynamics of the ith and lth nodes of the first layer are governed by the following ordinary differential equations:

$$\dot{\mathbf{x}}_1 = \dot{\mathbf{x}}_{1,i} = f(\mathbf{x}_1) + k_A \sum_{j=1}^{N} \tilde{\mathscr{A}}_{ij}^{[1]} G[\mathbf{x}_1, \mathbf{x}_1] + k_R H[\mathbf{x}_2, \mathbf{x}_1],$$

$$\dot{\mathbf{x}}_1 = \dot{\mathbf{x}}_{1,l} = f(\mathbf{x}_1) + k_A \sum_{j=1}^{N} \tilde{\mathscr{A}}_{lj}^{[1]} G[\mathbf{x}_1, \mathbf{x}_1] + k_R H[\mathbf{x}_2, \mathbf{x}_1]. \tag{11}$$

Subtracting these two equations, we obtain

$$\sum_{j=1}^{N} \left(\tilde{\mathscr{A}}_{ij}^{[1]} - \tilde{\mathscr{A}}_{lj}^{[1]}\right) G[\mathbf{x}_1, \mathbf{x}_1] = 0. \tag{12}$$

Similarly, the dynamics of the ith and lth nodes of the second layer yield the following equation:

$$\sum_{j=1}^{N} \left(\tilde{\mathscr{A}}_{ij}^{[2]} - \tilde{\mathscr{A}}_{lj}^{[2]}\right) G[\mathbf{x}_2, \mathbf{x}_2] = 0. \tag{13}$$

Since both the two chosen nodes i and l are arbitrary, thus the necessary condition for the intralayer synchronization gives the following criteria:

(1) $\sum_{j=1}^{N} \mathscr{A}_{ij}^{[\alpha]} = \sum_{j=1}^{N} \mathscr{A}_{lj}^{[\alpha]}$, $\alpha = 1, 2$, i.e., the in-degree of each node in the each layer must be equal or

(2) $G[\mathbf{x}_\alpha, \mathbf{x}_\alpha] = 0$, $\alpha = 1, 2$, i.e., the intralayer coupling function G vanishes after the oscillators of each layer evolve synchronously.

IV. RESULTS

For numerical simulations, we utilize a FORTRAN 90 compiler. We integrate Eq. (3) using the fifth-order Runge-Kutta-Fehlberg method with integration time step $h = 0.01$. As per our derived necessary conditions on the interlayer antisynchronization, H needs to be an odd function. Hence, we choose $H(\mathbf{x}_i, \mathbf{x}_j) = [x_j + x_i, y_j + y_i]^T$ where T represents the transpose of a vector. Similarly, the necessary conditions for the intralayer synchronization reveal either the in-degree of each node of the intralayer network is equal or G should vanish after the intralayer synchronization is achieved. Hence, we choose $G(\mathbf{x}_i, \mathbf{x}_j) = [x_j - x_i, y_j - y_i]^T$ as in the form of the linear diffusive coupling, so that G will become identically zero after achieving the intralayer synchronization state. The diffusive coupling was previously used in many systems [64], which removes the restriction on the intralayer network connectivity. This choice of G will allow us to choose any connected intralayer network.

A. Stuart-Landau oscillators

We first choose identical Stuart-Landau (SL) oscillators [65] to begin our numerical investigations. The state dynamics

of the limit cycle oscillator situated on top of the i-th node is represented by

$$f(\mathbf{x}_i) = \begin{pmatrix} [1 - (x_i{}^2 + y_i{}^2)]x_i - \omega_i y_i \\ [1 - (x_i{}^2 + y_i{}^2)]y_i + \omega_i x_i \end{pmatrix}, \qquad (14)$$

where $\mathbf{x}_i \in \mathbb{R}^2$. Since we are basically interested in the interlayer antisynchronization and intralayer synchronization, thus we choose the same intrinsic frequency $\omega_i = \omega = 3$ for all oscillators. Clearly, this f, being the odd function, satisfies the necessary condition for the emergence of the interlayer antisynchronization state.

1. Amplitude of each oscillator maintaining interlayer antisynchronization and intralayer synchronization

We analytically calculate the amplitude of each SL oscillator when each oscillator in a single layer undergoes a synchronous evolution with all the other units of the same layer, and simultaneously, each oscillator maintains an anti-synchronization state with all its replicas in different layers. The chosen functions G and H help us to write the dynamical evolution of each lth SL oscillator ($l = 1, 2, \ldots, N$) in the αth layer ($\alpha = 1, 2$) in terms of the complex variable $z_{\alpha,l} = x_{\alpha,l} + k y_{\alpha,l} = r_{\alpha,l} e^{k\theta_{\alpha,l}} \in \mathbb{C}$ as follows:

$$\dot{z}_{1,l} = (1 - |z_{1,l}|^2)z_{1,l} + k\omega z_{1,l} + k_A \sum_{j=1}^{N} \mathscr{\tilde{A}}_{lj}^{[1]}(z_{1,j} - z_{1,l}) + k_R(z_{2,l} + z_{1,l}),$$

$$\dot{z}_{2,l} = (1 - |z_{2,l}|^2)z_{2,l} + k\omega z_{2,l} + k_A \sum_{j=1}^{N} \mathscr{\tilde{A}}_{lj}^{[2]}(z_{2,j} - z_{2,l}) + k_R(z_{1,l} + z_{2,l}), \qquad (15)$$

where $k = \sqrt{-1}$, $r_{\alpha,l} = \sqrt{x_{\alpha,l}^2 + y_{\alpha,l}^2}$ is the amplitude of the SL oscillator situated in the lth node of the αth layer and the phase of that SL oscillator, $\theta_{\alpha,l}$ is given by the principal value of argument of the complex number $z_{\alpha,l}$, i.e., $\theta_{\alpha,l} = \tan^{-1}\left(\frac{y_{\alpha,l}}{x_{\alpha,l}}\right)$. By substituting $z_{1,l} = r_{1,l} e^{k\theta_{1,l}}$ and $z_{2,l} = r_{2,l} e^{k\theta_{2,l}}$ in (15), we find the phase of the oscillators obeys the following ordinary differential equations:

$$\dot{\theta}_{1,l} = \omega + k_A \sum_{j=1}^{N} \mathscr{\tilde{A}}_{lj}^{[1]} \frac{r_{1,j}}{r_{1,l}} \sin(\theta_{1,j} - \theta_{1,l})$$
$$+ k_R \frac{r_{2,l}}{r_{1,l}} \sin(\theta_{2,l} - \theta_{1,l}),$$

$$\dot{\theta}_{2,l} = \omega + k_A \sum_{j=1}^{N} \mathscr{\tilde{A}}_{lj}^{[2]} \frac{r_{2,j}}{r_{2,l}} \sin(\theta_{2,j} - \theta_{2,l})$$
$$+ k_R \frac{r_{1,l}}{r_{2,l}} \sin(\theta_{1,l} - \theta_{2,l}). \qquad (16)$$

In order to obtain these equations, we assume $r_{\alpha,l} \neq 0$, $l = 1, 2, \ldots, N$ and $\alpha = 1, 2$. Clearly, if $r_{\alpha,l} = 0$, then the system converges to the origin giving rise to the amplitude death state [66–69]. Hence for $r_{\alpha,l} = 0$, we can not anticipate interlayer antisynchronization state. Thus, we neglect the case of $r_{\alpha,l} = 0$. Similarly, we derive the rate of change of amplitude of the lth SL oscillator as follows:

$$\dot{r}_{1,l} = (1 - r_{1,l}^2)r_{1,l} + k_A \sum_{j=1}^{N} \mathscr{\tilde{A}}_{lj}^{[1]}[r_{1,j}\cos(\theta_{1,j} - \theta_{1,l}) - r_{1,l}]$$
$$+ k_R[r_{2,l}\cos(\theta_{2,l} - \theta_{1,l}) + r_{1,l}],$$

$$\dot{r}_{2,l} = (1 - r_{2,l}^2)r_{2,l} + k_A \sum_{j=1}^{N} \mathscr{\tilde{A}}_{lj}^{[2]}[r_{2,j}\cos(\theta_{2,j} - \theta_{2,l}) - r_{2,l}]$$
$$+ k_R[r_{1,l}\cos(\theta_{1,l} - \theta_{2,l}) + r_{2,l}]. \qquad (17)$$

For complete intralayer synchronization state, we have

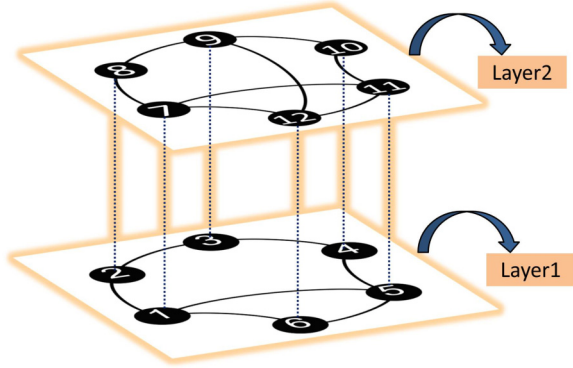$$r_{\alpha,i} = r_\alpha, \qquad \theta_{\alpha,i} = \theta_\alpha \qquad (18)$$

FIG. 1. A multiplex network: We here visualize a duplex network (a multiplex network with two layers) with the help of Gephi [70]. Each of these layers consists of a connected intralayer network. This network used for the numerical experiments (unless stated otherwise) contains 12 nodes and 21 links. The six interlayer edges (dotted lines) connect the replica nodes and help to connect the two connected layers.

for $\alpha = 1, 2$ and $i = 1, 2, \dots, N$.

Furthermore, if the system evolves in the interlayer antisynchronization state, then we have

$$r_1 = r_2, \quad \theta_1 - \theta_2 = \pm\pi. \tag{19}$$

Using Eqs. (18) and (19), Eq. (17) becomes

$$\dot{r}_1 = (1 - r_1^2) r_1. \tag{20}$$

Thus, the duplex networks in the presence of intralayer synchronization and interlayer antisynchronization states can be described by Eq. (20), where the local dynamics of each node are associated with the SL oscillator (14). Solving Eq. (20) as a function of time t, we have

$$r_1 = +\sqrt{\frac{e^{2t}}{e^{2t} - c_1}}. \tag{21}$$

Here c_1 is the integration constant. Also, the linear stability analysis of (20) suggests there are two stationary points: $r_1 = 0$ and $r_1 = 1$. The stationary point $r_1 = 0$ is unstable. In fact, we are not interested in $r_1 = 0$, as $r_1 = 0$ corresponds to the amplitude death state, which contradicts the emergence of the interlayer antisynchronization state. The other stationary point $r_1 = 1$ is stable. Thus, the system (15) experiencing the intralayer synchronization and the interlayer antisynchronization possesses the unit amplitude ($r_1 = 1$) irrespective of the choice of the coupling coefficients k_A and k_R.

2. Numerical illustration and demultiplexing effect

To validate our analytical findings, we consider the multiplex network given in Fig. 1. This multiplex network contains two layers, where each layer consists of two different connected intralayer networks. The first layer contains six nodes and seven links, whereas the second layer is made of six nodes and eight edges. On top of each of these vertices, we place identical SL oscillators (14) with the same intrinsic frequency $\omega = 3.0$. To verify our findings, here we propose two different measures:

(1) The first one

$$F_{\text{Replica}} = \left\langle \frac{1}{N} \sum_{i=1}^{N} [1 + \cos(\theta_{1,i} - \theta_{2,i})] \right\rangle \tag{22}$$

is to measure the interlayer antisynchronization. $\langle \cdot \rangle$ represents here the time average, and for numerical simulation, we choose 0.5×10^5 steps to average this measure after the initial transients of 1.5×10^5 steps. The scaling factor $\frac{1}{N}$ accounts for the N number of interlayer links. We are basically interested with only two values of F_{Replica}, viz. $F_{\text{Replica}} = 2$, which indicates the interlayer phase synchronization, and $F_{\text{Replica}} = 0$ representing the interlayer antisynchronization. However, this measure deals with only the phase of each oscillator; thus, to ensure the intralayer synchronization and interlayer antisynchronization, we need to see the temporal evolution of the state vectors too.

(2) To measure intralayer phase synchronization, we define

$$F_{\text{Layer1}} = \left\langle \frac{1}{L_1} \sum_{i<j} \mathscr{A}_{ij}^{[1]} [1 + \cos(\theta_{1,i} - \theta_{1,j})] \right\rangle,$$

$$F_{\text{Layer2}} = \left\langle \frac{1}{L_2} \sum_{i<j} \mathscr{A}_{ij}^{[2]} [1 + \cos(\theta_{2,i} - \theta_{2,j})] \right\rangle. \tag{23}$$

Here L_1 and L_2 are the numbers of edges of both connected layers, respectively. If these two measures attain their respective maximum values of 2, the system achieves intralayer phase synchronization. Besides, if they both acquire their respective minimum values 0, the system reaches intralayer antiphase synchronization.

Using the multiplex network in Fig. 1, we have construct the adjacency matrix $\mathscr{A}$ [see (5)]. The degree of each node is given by $d_1 = d_5 = d_7 = d_9 = d_{11} = d_{12} = 4$ and $d_2 = d_3 = d_4 = d_6 = d_8 = d_{10} = 3$. Using these degrees d_i and intralayer graphs, we construct the weighted directed networks with adjacency matrices $\mathscr{A}^{[\alpha]}$, $\alpha = 1, 2$. In Fig. 2 we plot the variation of F_{Layer1}, F_{Layer2}, and F_{Replica} by numerically integrating Eqs. (3) with intralayer coupling strength $k_A = 0.1$. For all the numerical simulations with identical SL oscillators, we choose initial conditions randomly for each oscillator within the interval $[-1, 1] \times [-1, 1]$. An exciting observation of Fig. 2 is that the system does not exhibit interlayer antisynchronization for any positive interlayer coupling coefficient k_R. Once the interlayer coupling strength k_R becomes negative and attains a sufficient value, F_{Replica} diminishes to zero and continues to be at zero, suggesting the occurrence of interlayer antisynchronization. To compare the results, we vary k_R within the interval $[-\frac{k_A}{10}, \frac{k_A}{10}]$ in each panel, where $k_A = 0.1$. We vary k_R from 0.01 to −0.01 with small space −0.0001, and for each step, we select the initial conditions randomly from $[-1, 1] \times [-1, 1]$. Figures 2(a)–2(c) are plotted for the hub-attracting intralayer matrix ($\beta = 1$), the unweighted intralayer matrix ($\beta = 0$), and the hub-repelling intralayer matrix ($\beta = -1$), respectively. Depending on the initial conditions in the small neighborhood of $k_R = 0$, F_{Replica} attains multiple values. However, the measures F_{Layer1} and F_{Layer2} reach their maximum values of 2 for all chosen values of the interlayer coupling strength k_R, even when k_R is negative. This suggests
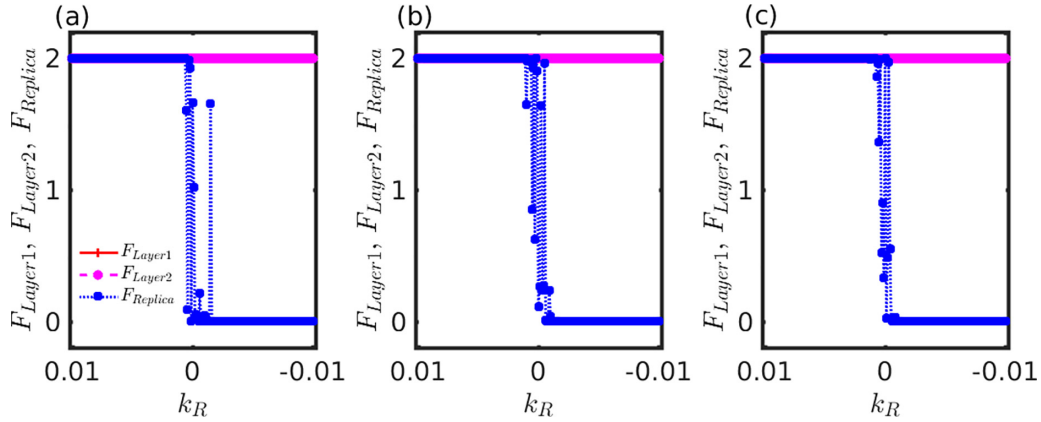
FIG. 2. The variation of F_{Layer1}, F_{Layer2}, and F_{Replica} as a function of interlayer coupling strength k_R: We choose the multiplex network shown in Fig. 1, and place an identical limit cycle oscillator (14) on top of each node with $\omega_i = \omega = 3$. We vary the interlayer coupling strength k_R from 0.01 to -0.01 with fixed space -0.0001 and fixed intralayer coupling strength $k_A = 0.1$. For each of these 200 k_Rs, we choose the initial condition of each oscillator randomly within the interval $[-1, 1] \times [-1, 1]$. For $k_R > 0$, the system remains in interlayer phase synchronization (i.e., $F_{\text{Replica}} = 2$) beyond a critical value of k_R. However, the system attains interlayer antisynchronization ($F_{\text{Replica}} = 0$) for a suitable negative interlayer coupling strength. Each of these subfigures is drawn with different adjacency matrices $\tilde{\mathscr{A}}^{[\alpha]}$ using the multiplex network in Fig. 1. Panel (a) represents the results for hub-attracting intralayer matrix ($\beta = 1$), whereas panel (c) depicts the results for the hub-repelling intralayer matrix ($\beta = -1$). The middle panel (b) shows the results for the unweighted intralayer matrix ($\beta = 0$). Irrespective of the chosen value of β, the system settles down to an interlayer antisynchronized state for negative interlayer coupling strength (see blue square markers). In spite of choosing negative k_R, each layer maintains intralayer synchronization as F_{Layer1} (red plus (+) markers) = F_{Layer2} (magenta circle markers) = 2 throughout the panels.

our chosen intralayer coupling strength k_A for this simulation is sufficient to maintain the coherent behavior among the identical SL oscillators within the layers, and the interlayer coupling strength k_R, even when it is negative, can not destroy the intralayer coherence. Nevertheless, for all these three matrices, F_{Replica} becomes zero beyond a critical value of $k_R < 0$. The required interlayer coupling strength with fixed $k_A = 0.1$ for the multiplex network given in Fig. 1 is as follows: (i) $k_R \approx -0.0037$ for hub-attracting intralayer matrix ($\beta = 1$), (ii) $k_R \approx -0.0033$ for unweighted intralayer matrix ($\beta = 0$), and (iii) $k_R \approx -0.0032$ for hub-repelling intralayer matrix ($\beta = -1$). All these critical values are obtained after averaging over 100 independent numerical simulations. We have the same underlying network structure in all these realizations but possess different random initial conditions. Thus, the critical interlayer coupling strength varies with each realization. Note that we do not want to emphasize the role of enhancement of interlayer antisynchronization here by changing the values of β. This topic is a subject of rigorous investigation and beyond the scope of the present work. The impact of β on the enhancement of interlayer antisynchronization and determine the critical value of k_R for different multiplex networks may be investigated in the near future. Nevertheless, we later perform the global stability analysis of the interlayer antisynchronization for a few special intralayer networks to elucidate the effect of initial conditions. i.e., we will determine an approximate value of interlayer coupling strength $k_R < 0$ for which the system evolves interlayer antisynchronously irrespective of the choice of initial conditions, except for a set of measure zero.

Thus, our selected intralayer coupling function G, interlayer coupling function H, intralayer coupling strength $k_A > 0$, and intralayer coupling strength $k_R < 0$ work immensely well for the emergence of intralayer synchronization and

interlayer antisynchronization states. However, as mentioned earlier, the proposed measures do not incorporate the amplitude of the oscillators. Hence, we plot the dynamics of each SL oscillator in Fig. 3. To avoid monotonicity, we show the results in Fig. 3 with only hub-attracting intralayer matrix ($\beta = 1$). Although we plot all 12 oscillators' temporal evolution in Fig. 3(a), however, we can only see two trajectories here. This is due to the simultaneous appearance of intralayer synchronization in both layers. All trajectories of the same layer collapse into a single one. To generate this figure, we choose the same multiplex network given in Fig. 1. We set the intralayer coupling strength $k_A = 0.1$ and the intralayer coupling strength $k_R = -0.1$, so that $|k_A| = |k_R|$. We again choose initial conditions randomly for each SL oscillator within the interval $[-1, 1] \times [-1, 1]$. Interestingly, the two intralayer synchronized trajectories maintain a constant π phase difference as revealed through Fig. 3(a). Apart from that, we also plot the sum $(x_{1,i} + x_{2,i})$ (see blue line) that indicates the sum of the dynamics of the oscillators situated on top of the replica nodes. This temporal evolution of $(x_{1,i} + x_{2,i})$ remains at zero after the initial transient as depicted in Fig. 3(a). This $(x_{1,i} + x_{2,i}) = 0$ suggests the emergence of interlayer antisynchronization. We also plot the positions of $x_{1,i}$ and $x_{2,i}$ of the multiplex at a particular time after the initial transient in Fig. 3(b). This snapshot indicates the occurrence of two synchronized clusters with π phase difference. Evidently, one of these synchronized clusters represents the state of the oscillators of one layer, and the other cluster reflects the dynamics of another layer. Figure 3(c) reveals any oscillator of the first layer (here, without any loss of generality, we choose $x_{1,1}$, i.e., the first oscillator) maintains a synchronized rhythm with any oscillator of the same layer (here we choose $x_{1,2}$, i.e., the second oscillator for visualization) and preserves the interlayer antisynchronization with the oscillators on top of the replica
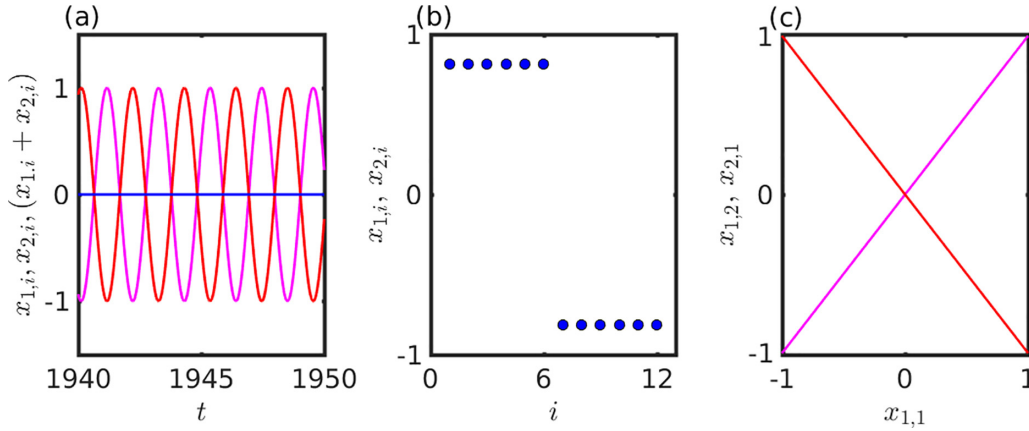
FIG. 3. Intralayer synchronization and interlayer antisynchronization for hub-attracting intralayer matrix ($\beta = 1$): All the trajectories of the first layer collapse to a single trajectory (red line), and similarly, the trajectories of the second layer oscillate within $[-1, 1]$ maintaining the same path (magenta line) in (a). This attests to the occurrence of intralayer synchronization. The sum $(x_{1,i} + x_{2,i})$ converges to a fixed value zero (blue line) after the transient. This validates the emergence of interlayer antisynchronization. Panel (b) contemplates the appearance of two clusters. The SL oscillators of the first layer lie within a synchronized group, and the oscillators of the second layer stay in another cluster. Due to the presence of repulsive interlayer coupling strength $k_R = -0.1$, these two clusters maintain a constant phase difference of π. All the panels are drawn using random initial conditions from $[-1, 1] \times [-1, 1]$. We choose the oscillators on top of the node 1, 2, and 7, respectively, from the multiplex network given in Fig. 1. We plot the phase portrait of these oscillators after the transient. Clearly, we have $x_{1,1} = x_{1,2} = -x_{2,1}$. More importantly, panels (a) and (c) confirm our analytical calculation revealing each SL oscillator evolves with a unit radius after reaching the interlayer antisynchronization manifold and the intralayer synchronization manifold. For each panel, we choose $k_A = |k_R| = 0.1$.

node of the other layer [see $x_{1,1} = -x_{2,1}$ in Fig. 3(c)]. Further, Figs. 3(a) and 3(c) ensure that the identical SL oscillators sustain a unit radius after achieving the intralayer synchronization and interlayer antisynchronization. This validates our analytical findings too.

Now we want to understand whether all these $N = 6$ interlayer links are necessary or not to achieve interlayer antisynchronization in the multiplex, chosen in Fig. 1. Instead of demultiplexing the multiplex randomly, we prefer a systematic way to demultiplex the network. First, we remove the connections between the first oscillator of both layers, i.e., we disconnect the interlayer link 1–7 of the multiplex shown in Fig. 1. Now, in the absence of this link 1–7, the network does not remain as a multiplex. However, it remains a multilayer network. Now, we integrate the system (3) by placing identical SL oscillators (14) on top of each node with $\omega = 3$. We choose the interlayer coupling strength $k_R = -0.1$ and set the intralayer coupling strength as $k_A = |k_R|$. We again choose the initial conditions randomly within $[-1, 1] \times [-1, 1]$. The chosen coupling strengths still allow the system to maintain the interlayer antisynchronization along with intralayer synchronization. Keeping the same coupling strengths and random initial conditions from $[-1, 1] \times [-1, 1]$, we remove the link 2–8 between the second oscillators of both layers. Interestingly, even this link removal does not destroy both the interlayer antisynchronization and intralayer synchronization. In fact, in this way, we gradually disconnect the interlayer links one by one. We find the system evolves in the interlayer antisynchronization and intralayer synchronization; still, there exists at least one interlayer link between the two layers. Unless we detach the last interlayer link 6–12, i.e., the connection between the sixth oscillators of both layers, the system settles in the interlayer antisynchronization state. Thus, only one interlayer link is sufficient to entertain the interlayer anti-

synchronization once the oscillators settle themselves into the intralayer synchronization manifold.

Here is a feasible explanation behind this occurrence of interlayer antisynchronization with only one interlayer link. Once the oscillators attain intralayer synchronization, this coherence will not be destroyed with negative interlayer coupling strength, as shown in Figs. 2 and 3. Thus, each of these two layers can be represented by two state vectors $\mathbf{x}_1(t)$ and $\mathbf{x}_2(t)$ (say), respectively. Now, since that one single interlayer link connects these two layers with repulsive interlayer coupling strength, thus these two state vectors $\mathbf{x}_1(t)$ and $\mathbf{x}_2(t)$ try to maximize their phase difference. Hence, we have $|\mathbf{x}_1(t)| = |\mathbf{x}_2(t)|$ and their phase difference is exactly π. In other words, we have $\mathbf{x}_1(t) + \mathbf{x}_2(t) = \mathbf{0}$. In Table I we represent how the gradual removal of interlayer links results in the values of F_{Layer1}, F_{Layer2}, and F_{Replica}. We find $F_{\text{Replica}} = 0$ until the single interlayer link 6–12 remains. After removing all interlayer links, F_{Replica} will give an initial condition-dependent value. Deleting all interlayer links still entertains the intralayer synchronization as the intralayer coupling strength $k_A = 0.1$ provides sufficient coherence among the oscillators within the same layer. Thus, we have $F_{\text{Layer1}} = F_{\text{Layer2}} = 2$ even without all interlayer connections.

B. Thomas' cyclically symmetric attractor

It is already established in Sec. III that the vector field f should be an odd function in order to realize one of the necessary conditions of interlayer antisynchronization along with intralayer synchronization. We already represent the results with the help of SL oscillators in the earlier subsection. To further validate our claim, we choose a different system with a self-excited attractor [71,72], *viz.*, Thomas' cyclically symmetric attractor [73–75], where the state dynamics of the

TABLE I. Demultiplexing of the network.

Removal of interlayer links	F_{Layer1}	F_{Layer2}	F_{Replica}
1–7	2	2	0
2–8	2	2	0
3–9	2	2	0
4–10	2	2	0
5–11	2	2	0
6–12	2	2	Initial condition-dependent value

ith oscillator is represented by

$$f(\mathbf{x}_i) = \begin{pmatrix} \sin(y_i) - bx_i \\ \sin(z_i) - by_i \\ \sin(x_i) - bz_i \end{pmatrix}, \tag{24}$$

where b is a constant. For $b > 1$, the origin is the single stable equilibrium. The system undergoes a pitchfork bifurcation at $b = 1$. As the parameter b is further decreased, the system undergoes a Hopf bifurcation around $b \approx 0.32899$, creating stable limit cycles. Through a period-doubling cascade, the system becomes chaotic at $b \approx 0.208186$.

We integrate Eqs. (6) with $\beta = -1$ by placing identical Thomas' cyclically symmetric attractor on top of each node. We simulate the system for 3×10^5 steps and discard the initial 2.7×10^5 steps treating them as transient. We choose the same coupling functions $G(\mathbf{x}_i, \mathbf{x}_j) = [x_j - x_i, y_j - y_i, z_j - z_i]^T$ and $H(\mathbf{x}_i, \mathbf{x}_j) = [x_j + x_i, y_j + y_i, z_j + z_i]^T$ for the numerical simulation. All the panels in Fig. 4 are drawn with fixed $k_A = 1.0$ and $k_R = -0.3$. We choose three distinct values of the system parameter b. All these panels suggest all the six oscillators of the same layer coincide in a single trajectory, indicating the intralayer synchronization. However, they exhibit replica-wise antiphase synchronization. We find $(x_{1,i} + x_{2,i})$ (blue line) converges to exactly zero after the initial transient in Fig. 4. Hence, we again confirm the emergence of the interlayer antisynchronization with Thomas' cyclically symmetric

attractor and validate our analytical calculations for such a state's existence.

V. LOCAL STABILITY ANALYSIS OF INTERLAYER ANTISYNCHRONIZATION STATE

We already derive a necessary condition

$$\sum_{j=1}^{N} \tilde{\mathscr{A}}_{ij}^{[1]} G[\mathbf{x}_{1,j}, \mathbf{x}_{1,i}] = -\sum_{j=1}^{N} \tilde{\mathscr{A}}_{ij}^{[2]} G[-\mathbf{x}_{1,j}, -\mathbf{x}_{1,i}] \tag{25}$$

for the emergence of interlayer antisynchronization. Still, now we ignore this condition as the function G is chosen as the diffusive function, and it will vanish identically after the occurrence of the intralayer synchronization. Therefore, the condition (25) mentioned above is trivially satisfied. Since G is chosen as, say, $G(\mathbf{x}_i, \mathbf{x}_j) = [x_j - x_i, y_j - y_i, z_j - z_i]^T = G[\mathbf{x}_i - \mathbf{x}_j]$. Thus from Eq. (25), we have

$$\sum_{j=1}^{N} \tilde{\mathscr{A}}_{ij}^{[1]} G[\mathbf{x}_{1,j} - \mathbf{x}_{1,i}] = -\sum_{j=1}^{N} \tilde{\mathscr{A}}_{ij}^{[2]} G[-\mathbf{x}_{1,j} + \mathbf{x}_{1,i}],$$

$$\Rightarrow \sum_{j=1}^{N} \tilde{\mathscr{A}}_{ij}^{[1]} G[\mathbf{x}_{1,j} - \mathbf{x}_{1,i}] = \sum_{j=1}^{N} \tilde{\mathscr{A}}_{ij}^{[2]} G[\mathbf{x}_{1,j} - \mathbf{x}_{1,i}]. \tag{26}$$
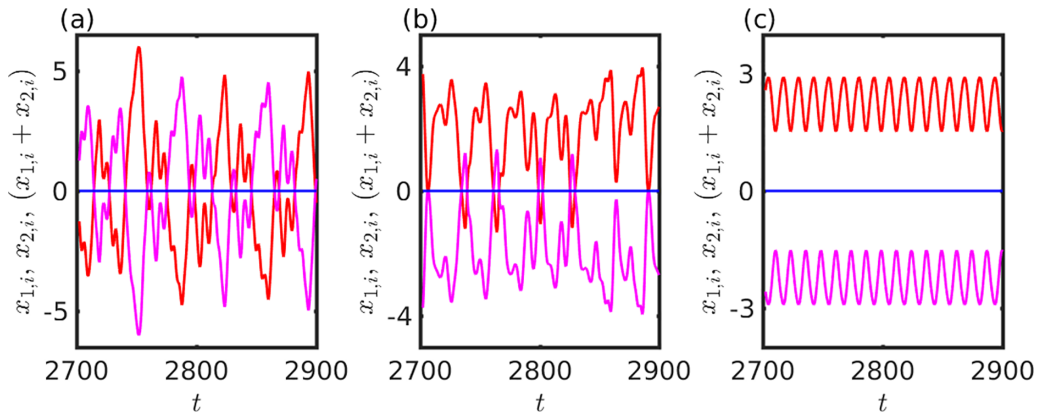

FIG. 4. The intralayer synchronization and intralayer antisynchronization with identical Thomas' cyclically symmetric attractor: The figures are drawn for (a) $b = 0.10$, (b) $b = 0.20$, and (c) $b = 0.30$. We consider the same multiplex network with 12 vertices and 21 edges, shown in Fig. 1. Initial conditions are chosen randomly from $[-4, 4] \times [-4, 4] \times [-4, 4]$. The interlayer coupling strength k_R is set at -0.3, and the intralayer coupling strength k_A is kept fixed at 1.0. We choose $\beta = -1$; thus, we have the hub-repelling intralayer matrices. In all panels, we find $(x_{1,i} + x_{2,i})$ converges to a fixed value zero after the initial transient. Hence, the emergence of interlayer antisynchronization is confirmed. Moreover, all the trajectories of the same layer collapse into a single trajectory [shown with the red (magenta) line for the first (second) layer].

The interlayer antisynchronization and the intralayer synchronization states are two completely independent emerging phenomena of a multiplex network. Thus, the system does not need to evolve into intralayer synchrony during the appearance of interlayer antisynchronization. Therefore, G may not vanish during the sole occurrence of interlayer antisynchronization. Hence for $G \neq 0$, we have from Eq. (26) the following simplistic choice:

$$\mathscr{A}^{[1]} = \mathscr{A}^{[2]} = \tilde{\mathscr{B}} \text{ (say)}. \qquad (27)$$

Thus, both connected layers contain the same intralayer networks. Hence, Eqs. (3) transform to the following set of equations:

$$\dot{\mathbf{x}}_{1,i} = f(\mathbf{x}_{1,i}) + k_A \sum_{j=1}^{N} \tilde{\mathscr{B}}_{ij} G[\mathbf{x}_{1,j} - \mathbf{x}_{1,i}]$$
$$+ k_R H[\mathbf{x}_{2,i} + \mathbf{x}_{1,i}],$$
$$\dot{\mathbf{x}}_{2,i} = f(\mathbf{x}_{2,i}) + k_A \sum_{j=1}^{N} \tilde{\mathscr{B}}_{ij} G[\mathbf{x}_{2,j} - \mathbf{x}_{2,i}]$$
$$+ k_R H[\mathbf{x}_{2,i} + \mathbf{x}_{1,i}]. \qquad (28)$$

During the occurrence of interlayer antisynchronization state, the synchronous solution satisfies

$$\dot{\mathbf{x}}_{1,i} = f(\mathbf{x}_{1,i}) + k_A \sum_{j=1}^{N} \tilde{\mathscr{B}}_{ij} G[\mathbf{x}_{1,j} - \mathbf{x}_{1,i}], \quad \dot{\mathbf{x}}_{2,i} = -\dot{\mathbf{x}}_{1,i}. \qquad (29)$$

Let $\delta\chi_i(t)$ be a tiny amount of feasible perturbation on the ith node of the second layer from its interlayer antisynchronization state. Then we have

$$\mathbf{x}_{2,i}(t) = -\mathbf{x}_{1,i}(t) + \delta\chi_i(t). \qquad (30)$$

Thus, the error dynamics transverse to the interlayer antisynchronization manifold $\Xi = \{(\mathbf{x}_{1,1}(t), \mathbf{x}_{1,2}(t), \ldots, \mathbf{x}_{1,N}(t)) \subseteq \mathbb{R}^{mN} : \mathbf{x}_{1,i}(t) + \mathbf{x}_{2,i}(t) = \mathbf{0}$ for all $i = 1, 2, \ldots, N$ and $t \in \mathbb{R}^+\}$ is given by the following equations:

$$\delta\dot{\chi}_i = \dot{\mathbf{x}}_{1,i} + \dot{\mathbf{x}}_{2,i}$$
$$= f(\mathbf{x}_{1,i}) + f(-\mathbf{x}_{1,i} + \delta\chi_i)$$
$$+ k_A \sum_{j=1}^{N} \tilde{\mathscr{B}}_{ij} G[\delta\chi_j - \delta\chi_i] + 2k_R H\delta\chi_i,$$
$$= Jf(\mathbf{x}_{1,i})\delta\chi_i - k_A \sum_{j=1}^{N} \tilde{\mathscr{L}}_{ij} G\delta\chi_j + 2k_R H\delta\chi_i, \qquad (31)$$

for all $i = 1, 2, \ldots, N$. Here $Jf(\mathbf{x}_{1,i}) = \frac{\partial f(\mathbf{x})}{\partial \mathbf{x}}|_{\mathbf{x}=\mathbf{x}_{1,i}}$, where $\mathbf{x}_{1,i}$ satisfies Eq. (29). Also, $\tilde{\mathscr{L}}$ be the zero-row sum intralayer Laplacian matrix [76], defined as $\mathscr{L}_{ij} = -\mathscr{B}_{ij}$ for $i \neq j$ and $\mathscr{L}_{ii} = \sum_{j=1}^{N} \mathscr{B}_{ij}$, $i = 1, 2, 3, \ldots, N$. Due to the linear independence of these error components, all the state variables of Eq. (31) evolve transverse to the interlayer antisynchronization manifold. Therefore, the Lyapunov exponents of Eq. (31) are all transverse to Ξ.

Now we place Thomas cyclically symmetric attractor on top of each node of the multiplex, and thus, using Eq. (31), we derive the following transverse error equations:

$$\delta\dot{x}_i = \cos(y_i)\delta y_i - b\delta x_i - k_A \sum_{j=1}^{N} \tilde{\mathscr{L}}_{ij}\delta x_j + 2k_R\delta x_i,$$
$$\delta\dot{y}_i = \cos(z_i)\delta z_i - b\delta y_i - k_A \sum_{j=1}^{N} \tilde{\mathscr{L}}_{ij}\delta y_j + 2k_R\delta y_i,$$
$$\delta\dot{z}_i = \cos(x_i)\delta x_i - b\delta z_i - k_A \sum_{j=1}^{N} \tilde{\mathscr{L}}_{ij}\delta z_j + 2k_R\delta z_i. \qquad (32)$$

For each $i = 1, 2, \ldots, N$, the state variable (x_i, y_i, z_i), being lying on the interlayer antisynchronization manifold, satisfies the following equations:

$$\dot{x}_i = \cos(y_i) - bx_i - k_A \sum_{j=1}^{N} \tilde{\mathscr{L}}_{ij}x_j,$$
$$\dot{y}_i = \cos(z_i) - by_i - k_A \sum_{j=1}^{N} \tilde{\mathscr{L}}_{ij}y_j,$$
$$\dot{z}_i = \cos(x_i) - bz_i - k_A \sum_{j=1}^{N} \tilde{\mathscr{L}}_{ij}z_j. \qquad (33)$$

Since we are interested in investigating the local stability of the interlayer antisynchronization state for the duplex network of Thomas cyclically symmetric attractor, we calculate $3N$ Lyapunov exponents by solving the linearized equation (32) along with the equation of motion (33) of the interlayer antisynchronization state. Out of these $3N$ Lyapunov exponents, the maximum Lyapunov exponent $\Lambda_{\max}$ will provide us the transition point from desynchronization to interlayer antisynchronization state. By keeping fixed the intralayer coupling strength k_A, we plot $\Lambda_{\max}$ as a function of the interlayer coupling strength k_R. $\Lambda_{\max} < 0$ will provide the necessary condition for the local stability of the interlayer antisynchronization state.

Similarly, if we place identical SL oscillators on top of each node of the multiplex instead of Thomas cyclically symmetric attractor, the error components transverse to the interlayer antisynchronization manifold satisfy the following evolution equation:

$$\delta\dot{x}_i = [1 - 3x_i^2 - y_i^2]\delta x_i - [\omega + 2x_iy_i]\delta y_i$$
$$- k_A \sum_{j=1}^{N} \tilde{\mathscr{L}}_{ij}\delta x_j + 2k_R\delta x_i,$$
$$\delta\dot{y}_i = (\omega - 2x_iy_i)\delta x_i + [1 - x_i^2 - 3y_i^2]\delta y_i$$
$$- k_A \sum_{j=1}^{N} \tilde{\mathscr{L}}_{ij}\delta y_j + 2k_R\delta y_i. \qquad (34)$$

For each $i = 1, 2, \ldots, N$, the state variable (x_i, y_i, z_i) of the interlayer antisynchronization state satisfies the following
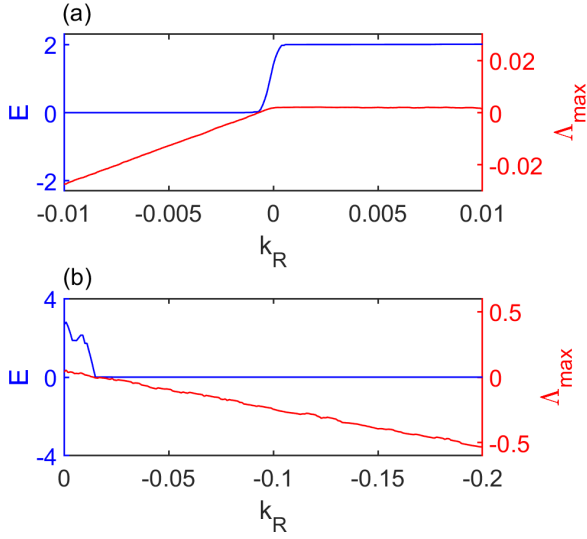
FIG. 5. The interlayer antisynchronization error E (blue) and the maximum transverse Lyapunov exponent $\Lambda_{\max}$ (red) as a function of the interlayer coupling strength k_R: Both layers contain the same ring intralayer network with four vertices. In (a) for the SL oscillator, we set the system's parameter at $k_A = 0.1$ and $\omega = 3.0$, whereas in (b) for the Thomas cyclically symmetric attractor, we set $k_A = 1.0$ and $b = 0.2$. E reduces to zero suggesting the occurrence of interlayer antisynchronization. Simultaneously, $\Lambda_{\max}$ crosses zero and becomes negative, revealing the appearance of interlayer antisynchronization. This indicates that our local stability condition agrees quite well with our numerical simulation.

equations:

$$\dot{x}_i = \left[1 - \left(x_i^2 + y_i^2\right)\right]x_i - \omega y_i - k_A \sum_{j=1}^{N} \tilde{\mathscr{L}}_{ij}x_j,$$

$$\dot{y}_i = \left[1 - \left(x_i^2 + y_i^2\right)\right]y_i + \omega x_i - k_A \sum_{j=1}^{N} \tilde{\mathscr{L}}_{ij}y_j. \quad (35)$$

For the computation of the maximum Lyapunov exponent $\Lambda_{\max}$ for the duplex of SL oscillators, we need to solve the linearized Eq. (34) along with Eq. (35) of the interlayer antisynchronization state, yielding the $2N$ Lyapunov exponents.

Figure 5 indicates our derived local stability condition works quite well. We choose the intralayer coupling strength $k_A = 0.1$ and the system parameter $\omega = 3.0$ for the SL oscillator in Fig. 5(a), whereas we keep fixed $k_A = 1.0$, and the system parameter $b = 0.2$ for the Thomas cyclically symmetric attractor in Fig. 5(b). We choose a ring network of four nodes in each layer for this simulation. As the constructed multiplex is a regular graph where the degree of each vertex of the multiplex is three, thus we have $\tilde{\mathscr{A}} = \mathscr{A}$ from Eq. (4). We plot the interlayer antisynchronization error E [see Eq. (8)] in Fig. 5 for both coupled systems. Clearly, E (blue) diminishes to zero gradually with the decrement of k_R. This $E = 0$ attests to the emergence of the interlayer antisynchronization state $\mathbf{x}_{1,i}(t) + \mathbf{x}_{2,i}(t) = \mathbf{0}$, $\forall\ i = 1, 2, 3, 4$. Similarly, the red lines in Fig. 5 contemplate the variation of the maximum Lyapunov exponent $\Lambda_{\max}$ as a function of k_R. As evident from Fig. 5, $\Lambda_{\max}$ becomes negative where E becomes zero in Fig. 5.

VI. SUFFICIENT CONDITION OF GLOBAL STABILITY ANALYSIS FOR INTERLAYER ANTISYNCHRONIZATION STATE

To derive the global stability condition for the interlayer antisynchronization state, we need to assume a few conditions which need to be satisfied for our calculations. If the following conditions are satisfied, our derived interlayer coupling strength k_R leads to the interlayer antisynchronization in the duplex network irrespective of the chosen initial conditions except for a set of measure zero.

(1) The first condition is the individual vector field f must be Lipschitz continuous, i.e., there exists a positive real constant M such that

$$\frac{\|f(\mathbf{x}) - f(\mathbf{y})\|}{\|\mathbf{x} - \mathbf{y}\|} \leqslant M, \quad \mathbf{x} \neq \mathbf{y}. \quad (36)$$

If the relation mentioned above holds, i.e., if there is an upper bound of the rate of change of the isolate oscillators' dynamics in the phase space, then capitalizing on the Cauchy-Schwarz inequality, we have

$$[\mathbf{x} - \mathbf{y}]^T[f(\mathbf{x}) - f(\mathbf{y})] \leqslant \|\mathbf{x} - \mathbf{y}\|\|f(\mathbf{x}) - f(\mathbf{y})\|$$
$$\leqslant M(\mathbf{x} - \mathbf{y})^T(\mathbf{x} - \mathbf{y})\forall \mathbf{x}, \mathbf{y} \in \mathbb{R}^m. \quad (37)$$

(2) The intralayer Laplacian matrix $\tilde{\mathscr{L}}$ must be a symmetric matrix. However, as per our construction, $\tilde{\mathscr{L}}$ is a symmetric matrix if and only if the intralayer network is a regular graph (i.e., $d_i = d_j$ for all i and j), or we choose $\beta = 0$, i.e., we consider only the unweighted case. Thus, we restrict our global stability analysis to two types of intralayer networks, viz., $\beta = 0$ or the regular intralayer networks where each node has the same degree. Hence under these two specific choices, the intralayer Laplacian matrix $\tilde{\mathscr{L}}$ is a symmetric positive semidefinite matrix. Thus, one of its eigenvalues is zero, and all the other eigenvalues are positive.

(3) The interlayer coupling matrix H must be a symmetric positive definite. Thus all of its eigenvalues are strictly positive.

(4) The intralayer coupling matrix G is a symmetric positive semidefinite matrix. Therefore all the eigenvalues of G are nonnegative.

Let us define the interlayer antisynchronization error for each replica as

$$\mathbf{e}_i = \mathbf{x}_{1,i} + \mathbf{x}_{2,i} \text{ for } i = 1, 2, \ldots, N. \quad (38)$$

Hence, we have

$$\dot{\mathbf{e}}_i = \dot{\mathbf{x}}_{1,i} + \dot{\mathbf{x}}_{2,i} = f(\mathbf{x}_{1,i}) + f(-\mathbf{x}_{1,i} + \mathbf{e}_i)$$
$$+ k_A \sum_{j=1}^{N} \tilde{\mathscr{B}}_{ij}G[\mathbf{e}_j - \mathbf{e}_i] + 2k_R H \mathbf{e}_i,$$
$$= f(\mathbf{x}_{1,i}) - f(\mathbf{x}_{1,i} - \mathbf{e}_i)$$
$$- k_A \sum_{j=1}^{N} \tilde{\mathscr{L}}_{ij}G\mathbf{e}_j + 2k_R H \mathbf{e}_i. \quad (39)$$

Let $\mathbf{e}$ be the stack of the error terms $\mathbf{e}_1, \mathbf{e}_2, \ldots, \mathbf{e}_N$ in the vectorial form. Then we can rewrite the rate of change of this

error system in the following form:

$$\dot{\mathbf{e}} = \bigoplus_{i=1}^{N}[f(\mathbf{x}_{1,i}) - f(\mathbf{x}_{1,i} - \mathbf{e}_i)] - k_A \tilde{\mathscr{L}} \otimes G\mathbf{e} + 2k_R I_N \otimes H\mathbf{e}, \tag{40}$$

where $\mathbf{x}_{1,i}$, $\mathbf{x}_{2,i}$ satisfy Eq. (28). Here $\bigoplus$ and $\otimes$ represent the matrix direct sum and Kronecker product, respectively.

Let us define a Lyapunov function in terms of the error quantities as

$$V(t) = \tfrac{1}{2}\mathbf{e}^T \mathbf{e}. \tag{41}$$

Then using Eq. (40), we have

$$\dot{V}(t) = \mathbf{e}^T \dot{\mathbf{e}} = \mathbf{e}^T \bigoplus_{i=1}^{N}[f(\mathbf{x}_{1,i}) - f(\mathbf{x}_{1,i} - \mathbf{e}_i)]$$

$$- k_A \mathbf{e}^T[\tilde{\mathscr{L}} \otimes G]\mathbf{e} + 2k_R \mathbf{e}^T[I_N \otimes H]\mathbf{e}$$

$$= \bigoplus_{i=1}^{N} \mathbf{e}_i^T[f(\mathbf{x}_{1,i}) - f(\mathbf{x}_{1,i} - \mathbf{e}_i)]$$

$$- k_A \mathbf{e}^T[\tilde{\mathscr{L}} \otimes G]\mathbf{e} + 2k_R \mathbf{e}^T[I_N \otimes H]\mathbf{e}. \tag{42}$$

To further proceed, we have to utilize the following boundedness of the quadratic form $\mathbf{x}^T D\mathbf{x}$, where $\mathbf{x}^T$ denotes the transpose of $\mathbf{x}$. Now if D is a real symmetric matrix of order N, then for all $\mathbf{x} \in \mathbb{R}^N$,

$$\lambda_{\min}[D]\mathbf{x}^T\mathbf{x} \leqslant \mathbf{x}^T D\mathbf{x} \leqslant \lambda_{\max}[D]\mathbf{x}^T\mathbf{x}, \tag{43}$$

where $\lambda_{\min}[D]$ and $\lambda_{\max}[D]$ are the minimum and maximum eigenvalues of D, respectively. These inequalities (37) and (43) help to convert Eq. (42) as follows:

$$\dot{V}(t) \leqslant [M - k_A\lambda_{\min}[\tilde{\mathscr{L}} \otimes G] + 2k_R\lambda_{\max}[I_N \otimes H]]\mathbf{e}^T\mathbf{e}. \tag{44}$$

Now, as per our assumption, G is a positive semidefinite matrix. Therefore all the eigenvalues of G are nonnegative. Also, the minimum eigenvalue of $\tilde{\mathscr{L}}$ is zero. Thus, we have

$$\lambda_{\min}[\tilde{\mathscr{L}} \otimes G] = \lambda_{\min}[\tilde{\mathscr{L}}]\lambda_{\min}[G] = 0. \tag{45}$$

Also, all the eigenvalues of I_N is 1. Thus, we have

$$\lambda_{\max}[I_N \otimes H] = \lambda_{\max}[H]. \tag{46}$$

Hence, Eq. (44) reduces to

$$\dot{V}(t) \leqslant [M + 2k_R\lambda_{\max}[H]]\mathbf{e}^T\mathbf{e}. \tag{47}$$

Since as per assumption, $\lambda_{\max}[H] > 0$. Thus, we know $\dot{V}(t) < 0$ yields the required global stability condition. Hence, Eq. (47) provides

$$k_R < -\frac{M}{2\lambda_{\max}[H]}. \tag{48}$$

Thus, whenever we choose an interlayer coupling strength k_R less than $\frac{-M}{2\lambda_{\max}[H]}$, the global stability of the interlayer antisynchronization state is assured irrespective of the chosen initial conditions (except for a set of measure zero) if our earlier mentioned assumptions hold. Note that the derived interlayer coupling strength is not optimized in the sense that it may be possible to calculate a better (optimal) interlayer

coupling strength to achieve such an interlayer antisynchronization state by introducing more higher-order error terms in the function (41). One more noticeable thing from the relation (48) is one needs negative interlayer coupling strength to establish the convergence of each oscillator in one layer anti synchronously to its counterpart oscillator on the other layer, irrespective of their initial conditions except for a set of measure zero. As per our specific choice of the interlayer coupling matrix $H = \text{diag}(1, 1, 1)$, we have $\lambda_{\max}[H] = 1$. Thus, the required interlayer coupling strength reduces to

$$k_R < -\frac{M}{2}. \tag{49}$$

Thus, our calculated interlayer coupling strength for the global convergence to the antisynchronization state of each replica node, irrespective of initial conditions, depends crucially on the Lipschitz constant of the isolated dynamics. Hence, one requires different coupling strengths for distinct dynamical systems. For instance, the Lipschitz constant for the SL oscillator with $\omega_i = \omega = 3$ is approximately 3.0. Similarly, the Lipschitz constant for the Thomas cyclically cylindrical oscillator with $b = 0.2$ is approximately 1.0711. Therefore, the required k_R for the global convergence of the replica-wise antisynchronization trajectories irrespective of initial conditions except for a set of measure zero is

$$k_R < -1.5$$

for the SL oscillators with the chosen system parameter as the local dynamics, and

$$k_R < -0.53555$$

for the Thomas cyclically cylindrical oscillators with the chosen system parameter as the local dynamics on top of the multiplex.

VII. DISCUSSION

It is noteworthy that one can map the interlayer antisynchronization problem into the interlayer synchronization by applying a suitable coordinate translation, $\mathbf{x}_{2,i} \to -\mathbf{x}'_{2,i}$. Definitely, such a transformation allows us to arrive at the standard synchronization problem; hence, we can use traditional techniques to study the phenomenon. However, by doing such a transformation, we will mathematically lose some valuable information about this phenomenon. Our derivations indicate that we need something extra apart from being identical for obtaining interlayer antisynchronization. Specifically, the oscillators should maintain symmetry in the form of an odd evolution function, which is necessary for achieving such a novel state. Furthermore, a few steps of calculations affirm that mathematically there are no restrictions in the interlayer coupling functions for maintaining interlayer complete synchronization in the translated coordinates. However, we successfully derive that one needs odd interlayer coupling functions to obtain interlayer antisynchronization.

Physically, we also lose the phenomenon of antisynchronization when we apply such a coordinate transformation, as the translated coordinates lead to the standard complete synchronization phenomenon. However, such a peculiar

VIII. SUMMARY AND REMARKS

The present article offers a thorough understanding of interlayer antisynchronization, a novel form of synchronization that emerges in multiplex networks with hub-attracting, hub-repelling, and unweighted intralayer networks. Our mathematics-inspired studies allow drawing a series of important conclusions about this unique dynamical phenomenon occurring in multiplex networks in terms of its local and global stability conditions, relation to network topology, coupling functions, and robustness under demultiplexing of the network. We have demonstrated that our analytically derived conditions for the existence and stability of such a solution agree perfectly well with numerical simulations. Further, we have derived a few necessary conditions analytically for the intralayer synchronization in multiplex networks and numerically verified it by assigning two different oscillators as the local dynamics at the top of the network's nodes. Apart from that, we successfully analytically predict the SL oscillators' amplitude during the simultaneous occurrence of interlayer antisynchronization and intralayer synchronization. Our results may serve as a starting point for unveiling the novel emergent collective dynamics in various natural systems. Although we are unaware of any immediate applications of the model studied here; however, our model may prove to be beneficial for studying the complex topological behavior of brain dynamics. References [100,101] demonstrate the usefulness of studying brain dynamics using multilayer networks, and smooth brain functioning depends crucially on the co-existence of excitatory and inhibitory neurons [102,103]. Examining the theoretical grounds of interlayer antisynchronization is essential in gaining some intuition about the cortical neuronal networks. We conclude with the hope that our systematic investigations with the theoretical framework may offer many possibilities for future research in generic multilayer networks, revealing far more fundamental aspects of these complex forms of synchronization.

antisynchronization state is worthy of investigation. For instance, Christiaan Huygens observed the opposite type of oscillation of two pendulums hanging from the same base in 1665 [64,77–79]. So, one can also map this phenomenon with "standard complete sync" in a translated coordinate system. But we know this is a particular type of "standard sync." Transforming the antiphase synchronization achieved by two pendulum clocks hanging on a common base into a synchronization phenomenon may solve the same problem mathematically, however, at the cost of losing the novel feature of the physical event.

Studying antiphase synchronization gained immense attention among researchers after the experiment by Huygens. For instance, Ref. [80] studies the existence and stabilization of various multi-cluster states, which may not be stable (even if it exists) in single-layer networks. References [81,82] investigated the partial synchronizations in the form of clusters in adaptively coupled phase oscillators. A numerical study of antiphase synchronization in a bilayer network of repulsively and bidirectionally coupled 2D lattices of van der Pol oscillators is furnished on Ref. [83]. Notably, the numerical study on van der Pol oscillators by Shepelev et al. supports our analytical findings too. Since its evolution function is an odd function, thus it is possible to observe interlayer antisynchronization in such a system. Using multiplex architectures in combination with attractive intralayer and repulsive interlayer connections, the antiphase synchronization of identical dynamical systems is analytically investigated in Ref. [19]. This study provides an elegant way of establishing antiphase synchronization in a multiplex network by introducing repulsive coupling through any spanning tree of a single connected layer and the interlayer links.

In fact, there are numerous investigations on antiphase synchronization [54,84–87] and antisynchronization [88–99]. However, our goal is to look at the interlayer antisynchronization of attractive-repulsively coupled amplitude oscillators in a multilayer network. And each of its layers may consist of a hub-attracting, hub-repelling, or unweighted network. The inclusion of diverse factors like (i) attractive-repulsive interaction, (ii) multilayer networks, (iii) amplitude oscillators, and (iv) hub-attracting, hub-repelling, and unweighted intralayer adjacency matrix, leads to a complex system, and despite the complexities of our proposed model, we can provide a few exciting outcomes of this novel form of synchronization, including (1) necessary conditions for the existence of intralayer synchronization and interlayer antisynchronization, (2) calculating the amplitude of each oscillator by analytically solving $2N$-coupled ordinary differential equations, (3) impact of demultiplexing, and (4) local and global stability analysis of interlayer antisynchronization state.

[1] M. Kivelä, A. Arenas, M. Barthelemy, J. P. Gleeson, Y. Moreno, and M. A. Porter, J. Complex Netw. **2**, 203 (2014).

[2] S. Boccaletti, G. Bianconi, R. Criado, C. I. Del Genio, J. Gómez-Gardenes, M. Romance, I. Sendina-Nadal, Z. Wang, and M. Zanin, Phys. Rep. **544**, 1 (2014).

[3] Z. Wang, L. Wang, A. Szolnoki, and M. Perc, Eur. Phys. J. B **88**, 1 (2015).

[4] Y.-Z. Chen, Z.-G. Huang, H.-F. Zhang, D. Eisenberg, T. P. Seager, and Y.-C. Lai, Sci. Rep. **5**, 17277 (2015).

[5] I. Hernandez-Fajardo and L. Dueñas-Osorio, Reliab. Eng. Syst. Safety **111**, 260 (2013).

[6] J. Gao, S. V. Buldyrev, H. E. Stanley, and S. Havlin, Nat. Phys. **8**, 40 (2012).

[7] S. V. Buldyrev, R. Parshani, G. Paul, H. E. Stanley, and S. Havlin, Nature (London) **464**, 1025 (2010).

[8] D. Helbing, Rev. Mod. Phys. **73**, 1067 (2001).

[9] R. G. Morris and M. Barthelemy, Phys. Rev. Lett. **109**, 128703 (2012).

[10] C. Granell, S. Gómez, and A. Arenas, Phys. Rev. Lett. **111**, 128701 (2013).

[11] J. Sanz, C.-Y. Xia, S. Meloni, and Y. Moreno, Phys. Rev. X **4**, 041005 (2014).

[12] G. Menichetti, L. Dall'Asta, and G. Bianconi, Sci. Rep. **6**, 1 (2016).

[13] J. Gómez-Gardenes, I. Reinares, A. Arenas, and L. M. Floría, Sci. Rep. **2**, 1 (2012).

[14] S. Nag Chowdhury, S. Kundu, M. Duh, M. Perc, and D. Ghosh, Entropy **22**, 485 (2020).

[15] S. Gomez, A. Diaz-Guilera, J. Gomez-Gardenes, C. J. Perez-Vicente, Y. Moreno, and A. Arenas, Phys. Rev. Lett. **110**, 028701 (2013).

[16] I. Leyva, R. Sevilla-Escoboza, I. Sendiña-Nadal, R. Gutiérrez, J. Buldú, and S. Boccaletti, Sci. Rep. **7**, 45475 (2017).

[17] S. Rakshit, B. K. Bera, and D. Ghosh, Phys. Rev. E **101**, 012308 (2020).

[18] I. Leyva, I. Sendiña-Nadal, R. Sevilla-Escoboza, V. Vera-Avila, P. Chholak, and S. Boccaletti, Sci. Rep. **8**, 8629 (2018).

[19] S. N. Chowdhury, S. Rakshit, J. M. Buldu, D. Ghosh, and C. Hens, Phys. Rev. E **103**, 032310 (2021).

[20] S. Rakshit, F. Parastesh, S. Nag Chowdhury, S. Jafari, J. Kurths, and D. Ghosh, Nonlinearity **35**, 681 (2021).

[21] L. V. Gambuzza, M. Frasca, and J. Gomez-Gardenes, EPL (Europhys. Lett.) **110**, 20010 (2015).

[22] S. Rakshit, B. K. Bera, E. M. Bollt, and D. Ghosh, SIAM J. Appl. Dyn, Syst. **19**, 918 (2020).

[23] M. S. Anwar and D. Ghosh, Chaos **32**, 033125 (2022).

[24] F. Della Rossa, L. Pecora, K. Blaha, A. Shirin, I. Klickstein, and F. Sorrentino, Nat. Commun. **11**, 3179 (2020).

[25] S. Jalan and A. Singh, EPL (Europhys. Lett.) **113**, 30002 (2016).

[26] X. Zhang, S. Boccaletti, S. Guan, and Z. Liu, Phys. Rev. Lett. **114**, 038701 (2015).

[27] S. Jalan, A. Kumar, and I. Leyva, Chaos **29**, 041102 (2019).

[28] P. Khanra, P. Kundu, C. Hens, and P. Pal, Phys. Rev. E **98**, 052315 (2018).

[29] V. H. Louzada, N. A. Araújo, J. S. Andrade, and H. J. Herrmann, Sci. Rep. **3**, 3289 (2013).

[30] S. Majhi, T. Kapitaniak, and D. Ghosh, Chaos **29**, 013108 (2019).

[31] C. I. Del Genio, J. Gómez-Gardeñes, I. Bonamassa, and S. Boccaletti, Sci. Adv. **2**, e1601679 (2016).

[32] D. Li and C. Zhou, Front. Syst. Neurosci. **5**, 100 (2011).

[33] L. M. Pecora and T. L. Carroll, Phys. Rev. Lett. **80**, 2109 (1998).

[34] L. Tang, X. Wu, J. Lü, J.-a. Lu, and R. M. D'Souza, Phys. Rev. E **99**, 012304 (2019).

[35] M. Kassabov, S. H. Strogatz, and A. Townsend, A global synchronization theorem for oscillators on a random graph, Chaos: Interdiscip. J. Non. Sci. **32**, 093119 (2022).

[36] S. Nag Chowdhury and D. Ghosh, EPL (Europhys. Lett.) **125**, 10011 (2019).

[37] A. Arenas, A. Díaz-Guilera, J. Kurths, Y. Moreno, and C. Zhou, Phys. Rep. **469**, 93 (2008).

[38] S. Nag Chowdhury, S. Majhi, D. Ghosh, and A. Prasad, Phys. Lett. A **383**, 125997 (2019).

[39] T. Wu, S. Huo, K. Alfaro-Bittner, S. Boccaletti, and Z. Liu, Phys. Rev. Res. **4**, 033009 (2022).

[40] S. Nag Chowdhury, A. Ray, A. Mishra, and D. Ghosh, J. Phys.: Complexity **2**, 035021 (2021).

[41] D. Ghosh, M. Frasca, A. Rizzo, S. Majhi, S. Rakshit, K. Alfaro-Bittner, and S. Boccaletti, Phys. Rep. **949**, 1 (2022).

[42] S. Chatterjee, S. Nag Chowdhury, D. Ghosh, and C. Hens, Chaos **32**, 103122 (2022).

[43] A. Mishra, C. Hens, M. Bose, P. K. Roy, and S. K. Dana, Phys. Rev. E **92**, 062920 (2015).

[44] C. R. Hens, O. I. Olusola, P. Pal, and S. K. Dana, Phys. Rev. E **88**, 034902 (2013).

[45] C. R. Hens, P. Pal, S. K. Bhowmick, P. K. Roy, A. Sen, and S. K. Dana, Phys. Rev. E **89**, 032901 (2014).

[46] B. K. Bera, C. Hens, and D. Ghosh, Phys. Lett. A **380**, 2366 (2016).

[47] P. Kundu, L. Sharma, M. Nandan, D. Ghosh, C. Hens, and P. Pal, Chaos **29**, 013112 (2019).

[48] C. Zhou, A. E. Motter, and J. Kurths, Phys. Rev. Lett. **96**, 034101 (2006).

[49] C. Zhou and J. Kurths, Phys. Rev. Lett. **96**, 164102 (2006).

[50] M. Chavez, D.-U. Hwang, A. Amann, and S. Boccaletti, Chaos **16**, 015106 (2006).

[51] L. Kempton, G. Herrmann, and M. Di Bernardo, IEEE Trans. Control Netw. Syst. **5**, 1541 (2017).

[52] I. Leyva, I. Sendina-Nadal, J. A. Almendral, A. Navas, S. Olmi, and S. Boccaletti, Phys. Rev. E **88**, 042808 (2013).

[53] S. Majhi, S. Nag Chowdhury, and D. Ghosh, EPL (Europhys. Lett.) **132**, 20001 (2020).

[54] S. N. Chowdhury, D. Ghosh, and C. Hens, Phys. Rev. E **101**, 022310 (2020).

[55] G. K. Sar, S. Nag Chowdhury, M. Perc, and D. Ghosh, New J. Phys. **24**, 043004 (2022).

[56] S. Nag Chowdhury, S. Majhi, M. Ozer, D. Ghosh, and M. Perc, New J. Phys. **21**, 073048 (2019).

[57] S. Nag Chowdhury, A. Ray, S. K. Dana, and D. Ghosh, Phys. Rep. **966**, 1 (2022).

[58] S. Nag Chowdhury, S. Majhi, and D. Ghosh, IEEE Trans. Netw. Sci. Eng. **7**, 3159 (2020).

[59] A. Girón, H. Saiz, F. S. Bacelar, R. F. Andrade, and J. Gómez-Gardenes, Chaos **26**, 065302 (2016).

[60] F. S. Bacelar, J. M. Calabrese, and E. Hernández-García, Ecol. Complex. **17**, 140 (2014).

[61] E. Estrada, Linear Algebra Appl. **596**, 256 (2020).

[62] L. V. Gambuzza, M. Frasca, and E. Estrada, SIAM J. Appl. Dyn. Syst. **19**, 1057 (2020).

[63] M. S. Anwar, D. Ghosh, and N. Frolov, Mathematics **9**, 2135 (2021).

[64] A. Pikovsky, M. Rosenblum, and J. Kurths, *Synchronization: A Universal Concept in Nonlinear Sciences*, Cambridge Nonlinear Science Series (Cambridge University Press, Cambridge, 2001).

[65] Y. Kuramoto, *Chemical Oscillations, Waves and Turbulence* (Dover Publications, Mineola, NY, 2003).

[66] G. Saxena, A. Prasad, and R. Ramaswamy, Phys. Rep. **521**, 205 (2012).

[67] S. Dixit, S. Nag Chowdhury, A. Prasad, D. Ghosh, and M. D. Shrimali, Chaos **31**, 011105 (2021).

[68] V. Resmi, G. Ambika, and R. E. Amritkar, Phys. Rev. E **84**, 046212 (2011).

[69] S. Dixit, S. Nag Chowdhury, D. Ghosh, and M. D. Shrimali, (EPL) Europhys. Lett. **133**, 40003 (2021).

[70] M. Bastian, S. Heymann, and M. Jacomy, Proc. Int. AAAI Conf. Social Media **3**, 361 (2009).

[71] D. Dudkowski, S. Jafari, T. Kapitaniak, N. V. Kuznetsov, G. A. Leonov, and A. Prasad, Phys. Rep. **637**, 1 (2016).

[72] S. Nag Chowdhury and D. Ghosh, Eur. Phys. J.: Spec. Top. **229**, 1299 (2020).

[73] R. Thomas, Intl. J. Bifurcat. Chaos **09**, 1889 (1999).

[74] J. C. Sprott and K. E. Chlouverakis, Intl. J. Bifurcat. Chaos **17**, 2097 (2007).

[75] G. Rowlands and J. Sprott, Phys. Plasmas **15**, 082308 (2008).

[76] M. S. Anwar, S. Kundu, and D. Ghosh, Chaos Solitons Fractals **142**, 110476 (2021).

[77] I. I. Blekhman, *Synchronization in Science and Technology* (ASME Press, New York, 1988).

[78] R. Dilão, Chaos **19**, 023118 (2009).

[79] J. Carranza, M. Brennan, and B. Tang, J. Phys. Conf. Ser. **744**, 012133 (2016).

[80] R. Berner, J. Sawicki, and E. Schöll, Phys. Rev. Lett. **124**, 088301 (2020).

[81] R. Berner, E. Scholl, and S. Yanchuk, SIAM J. Appl. Dyn. Syst. **18**, 2227 (2019).

[82] R. Berner, J. Fialkowski, D. Kasatkin, V. Nekorkin, S. Yanchuk, and E. Schöll, Chaos **29**, 103134 (2019).

[83] I. A. Shepelev, S. S. Muni, E. Schöll, and G. I. Strelkova, Chaos **31**, 063116 (2021).

[84] I. Shepelev, A. Bukh, G. Strelkova, and V. Anishchenko, Chaos Solitons Fractals **143**, 110545 (2021).

[85] W. Liu, J. Xiao, X. Qian, and J. Yang, Phys. Rev. E **73**, 057203 (2006).

[86] S. Nazhan and Z. Ghassemlooy, Appl. Opt. **58**, 9491 (2019).

[87] A. D. Kachhvah and S. Jalan, Phys. Rev. E **105**, L062203 (2022).

[88] G.-H. Li and S.-P. Zhou, Chaos Solitons Fractals **32**, 516 (2007).

[89] M. Yuan, W. Wang, X. Luo, L. Liu, and W. Zhao, Chaos Solitons Fractals **113**, 244 (2018).

[90] S. Zhangyi, W. Linli, Z. Yongxin, and H. Imani, Intl. J. Model. Simul., 1 (2022).

[91] T. Khan and H. Chaudhary, Numer. Algebr. Control. Optim. **12**, 611 (2021).

[92] E. E. Mahmoud, P. Trikha, L. S. Jahanzaib, M. Higazy, and M. H. Alkinani, Adv. Differ. Eq. **2021**, 1 (2021).

[93] L. Chen, C. Huang, H. Liu, and Y. Xia, Mathematics **7**, 559 (2019).

[94] V. R. Gowse, B. Palanivel, and S. Sivaprakasam, arXiv:1805.01122.

[95] M. M. Al-Sawalha, M. Noorani, and M. Al-Dlalah, Comput. Math. Appl. **59**, 3234 (2010).

[96] S. Vaidyanathan and K. Rajagopal, *Proceedings of the Advances in Computing and Information Technology: First International Conference, ACITY 2011, Chennai, India, July 15–17, 2011* (Springer, Berlin, Heidelberg, 2011), pp. 175–184.

[97] Y. Wu, L. Liu, J. Hu, and G. Feng, IEEE Trans. Neural Netw. Learn. Syst. **29**, 807 (2017).

[98] F. Liu, W. Meng, and D. Yao, IEEE Trans. Neural Netw. Learn. Syst. (to be published).

[99] S. K. Bhowmick, C. Hens, D. Ghosh, and S. K. Dana, Phys. Lett. A **376**, 2490 (2012).

[100] M. De Domenico, Giga Sci. **6**, gix004 (2017).

[101] J. M. Buldú and M. A. Porter, Netw. Neurosci. **2**, 418 (2018).

[102] J. Soriano, M. Rodríguez Martínez, T. Tlusty, and E. Moses, Proc. Natl. Acad. Sci. USA **105**, 13758 (2008).

[103] T. P. Vogels and L. Abbott, Nat. Neurosci. **12**, 483 (2009).